Article ID: 1003－6326(2005)01－0035－05

Cavitation-erosion mechanism of laser cladded SiC particle reinforced metal matrix composite①

ZHANG Chun-hua(张春华)[1, 2, 3], ZHANG Song(张 松)[1], YANG Hong-gang(杨洪刚)[1], ZHU Sheng-long(朱圣龙)[2], MAN Hau-chung(文效忠)[4], CAI Qing-kui(才庆魁)[3]

(1. College of Materials Science & Engineering, Shenyang University of Technology, Shenyang 110023, China;
2. State Key Lab for Corrosion & Protection, The Chinese Academy of Sciences, Shenyang 110016, China;
3. College of Materials & Metallurgy, Northeastern University, Shenyang 110004, China;
4. Department of Industrial & Systems Engineering, Hong Kong Polytechnic University, Hong Kong, China)

Abstract: With 2 kW continuous wave Nd-YAG laser, SiC ceramic powder was laser-cladded on the AA6061 aluminium alloy surface. Within the range of process parameters investigated, the parameters were optimized to produce the SiC_p reinforced metal matrix composites(MMC) modified layer on AA6061 alloy surface. After being treated, the modified layer is crack-free, porosity-free, and has good metallurgical bond with the substrate. The microstructure and chemical composition of the modified layer were analyzed by such detection devices as scanning electronic microscope(SEM-EDX) and X-ray diffractometer(XRD). The performance of electrochemical corrosion and cavitation erosion and their mechanism were estimated by the microhardness tester, potentiostat and ultrasonic-induced cavitation device.

Key words: aluminium alloy; laser-cladding; particle reinforced metal matrix composite; cavitation erosion

CLC number: TN 249 **Document code:** A

1 INTRODUCTION

Because of its good physical and chemical characteristics, aluminium alloy is widely used in aviation, astronavigation and power generating machine. But due to its low hardness and poor resistance to wear, aluminium alloy has difficulty to be used in the case of wear-erosion and abrasion. Conventional heat-treatment methods, for example, surface quenching, solution strengthening, chemical heat-treatment, are limited to improve the surface performance of aluminium alloy. Recently, there are some reports about the application of high-energy laser-cladding on the surface of aluminium matrix composites to improve the ability of the resistance to erosion and wear[1-5].

Cavitation erosion is a peculiar form of wear. It is caused by the high-speed relative movement between the fluid and metal structural unit, which produces the eddy that is accompanied by the bubble appearing and vanishing on the surface of metal in the local metal surface. Because the cavitation-erosion is the outcome of the combined action of the changed stress and erosion media, it accelerates the destroying-speed of the metal so that it brings serious damage and enormous economic loss to the lives of people and industrial production. As we all know, aluminium alloy is one of the materials that have poor cavitation-erosion and wear resistance, so plastic yield and ductile rupture can easily appear under the condition of cavitation-erosion[6].

Aluminium alloy has low absorptive power for the laser and ineffective phase transformation strengthening when irradiated by laser. Under the given conditions, the surface performance of the aluminium alloy can be effectively improved by the formation of SiC ceramic particle reinforced metal matrix composite(MMC) modified layer which has pre-pasted on the surface and then irradiated by laser. The purpose of this paper is to study the microstructure and cavitation-erosion behavior of the SiC particle reinforced MMC.

2 EXPERIMENTAL

2.1 Composition of substrate and alloy powder

① **Foundation item:** Project(2002AA305203) supported by Hi-tech Research and Development Program of China; Project(20031024) supported by Liaoning Scientific and Technological Development Foundation; Project(2004D011) supported by Liaoning Educational Committee Research Plan **Received date:** 2004－03－03; **Accepted date:** 2004－10－18

Correspondence: ZHANG Chun-hua, Associate professor, PhD; Tel: +86-24-25694821; Fax: +86-24-25691768; E-mail: songzhang_sy@yahoo.com.cn

AA6061 aluminium alloy with T6 treatment was used as the substrate material. The nominal chemical composition(in mass fraction, %) of this alloy is: 0.4-0.8Si, 0.7Fe, 0.15-0.4Cu, 0.15Mn, 0.8-1.2Mg, 0.04-0.35Cr, 0.25Zn, 0.15Ti and balance Al. The material was machined into specimen blocks of 40 mm × 40 mm × 10 mm. SiC ceramic powder is of industrial purity and the grain size is 43 - 104 μm. Table 1 lists the physical properties of AA6061Al alloy matrix and SiC.

Table 1 Physical property of AA6061 alloy matrix and SiC

Material	Density/ ($g \cdot cm^{-3}$)	Elastic modulus/ GPa	Tensile strength/ MPa	Melting point/ ℃
AA6061	2.7	70	70 - 600	660
SiC	3.22	410	200 - 500	2 400

2.2 Laser-cladding experiment

The Al alloy specimens were sand-blasted and rinsed to achieve a consistent surface roughness of R_a= 0.2 μm. SiC powder was made into the paste by agglomerant and was then painted evenly onto the rough specimen surface. The painted specimen was then dried in an oven at 120 ℃ for 4 h. The thickness of the pre-pasted SiC powder on the surface of Al alloy was 0.2 mm. The process parameters of the continuous wave Nd-YAG solid laser were: power 1 200 W, diameter of beam 2.5 mm, scanning speed 5 mm/s, flux of argon shield 20 L/min.

2.3 Electrochemical-corrosion and cavitation-erosion test

The dimension of the specimens for electrochemical-corrosion and cavitation-erosion tests is 13 mm × 13 mm × 10 mm. The square surface of 13 mm × 13 mm is used to be laser-cladded. The specimens were polished to a constant surface roughness using 1 μm diamond paste and then cleaned, degreased and dried.

The electrochemical polarization curve was set out by EG&G PARC273 corrosion system according to ASTM Standard G61—86[7], which can be used to value the performance of electrochemical corrosion resistance. The 3.5% NaCl solution was maintained at (23 ±1) ℃ during the test. Before test, N_2 was blown into solution in order to remove the air in it. A saturated calomel electrode (SCE) was used as the reference electrode to measure the performance of corrosion. The electric potential was increased from 200 mV below the anode corrosion potential at a scanning rate of 1 mV/s. When anode current is 10^{-2} A/cm^2, the potential scanning direction was reversed to determine the protecting potential under this corrosion system.

Cavitation erosion experiments were carried out using an ultrasonic-induced cavitation facility with a 550 W ultrasonic probe corresponding to ASTM Standard G32—92[8]. Fig. 1 shows the schematic diagram of cavitation erosion test. Between the stationary specimen and the vibrating 316L stainless steel stud was kept at 1 mm. The surface of the stainless steel stud was polished by 1 μm diamond paste in every intermittent period of 30 min in order to keep a constant surface roughness. The vibration frequency and peak-to-peak amplitude were 20 kHz and 30 μm, respectively. The specimens were subjected to a series of cavitation erosion tests in 3.5% NaCl solution and the temperature of the solution was kept at 23 ℃ by a chiller. Each cavitation erosion test was completed after 4 h, which included eight intermittent periods with each period of 30 min.

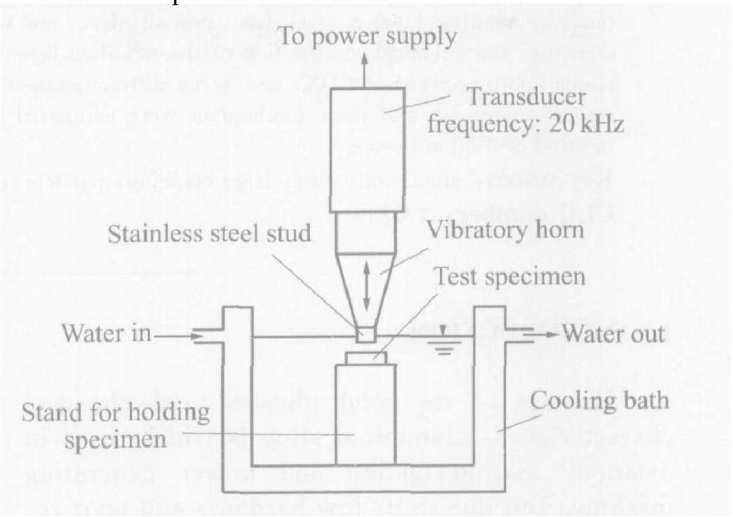

Fig. 1 Schematic diagram of cavitation-erosion testing

The mass loss of the specimens by cavitation erosion was measured by an electronic beam balance with an accuracy of ±0.1 mg. The cavitation erosion rate was calculated by

$$r_C = \frac{\Delta m}{A\ \Delta t} \quad (1)$$

where Δm is the accumulative mass loss of the specimen at some time, mg; A is the surface area of the specimen, cm^2; Δt is time of cavitation corrosion, h.

The surface microstructure and chemical composition of the specimen that have been laser-cladded and cavitation-eroded were analyzed by SEM and EDX. The hardness was measured by Shimadzu microhardness tester with 2 N(0.2 kg) loading for 15 s. Make use of XRD to analyze the phase structure of the laser surface cladded. The radiation used in XRD was Cu K_α with nickel filter and generated at 40 kV and 35 mA. The scanning rate used was 1.5(°)/min.

3 RESULTS AND DISCUSSION

3.1 Microstructure of laser-cladded surface

Fig. 2 shows the optical micrograph of the laser-cladded surface and illustrates the high integrity, porosity-free, crack-free characteristic and good bond between laser cladded surface and substrate. SiC particle is evenly distributed on the MMC with an average particle size of 15 μm. The high percentage of SiC particle reinforced phase is obtained on the layer of the specimen.

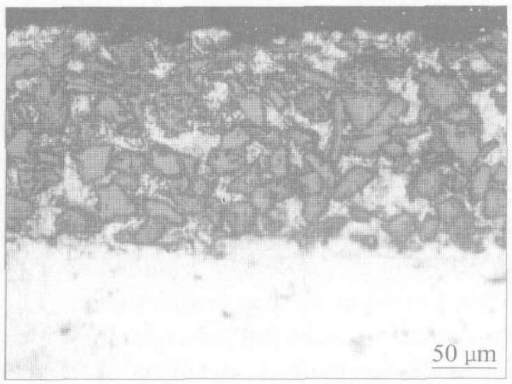

Fig. 2 Microstructure of laser cladded layer

The surface of the aluminium alloy was molten by the laser beam energy absorbed during the process of laser irradiation. The absorbing rate of materials for laser beam was determined by the electric resistance of specimen and wavelength of the laser beam which can be expressed as follows[9]:

$$\alpha(T) = 0.365\{\rho_{20}[1+\beta(T-293)]/\lambda\}^{0.5} - 0.0667\{\rho_{20}[1+\beta(T-293)]/\lambda\} + 0.006\{\rho_{20}[1+\beta(T-293)]/\lambda\}^{1/5} \quad (2)$$

where α is absorbing rate of the material; ρ is electric resistance ratio, Ω·cm; λ is wavelength of the incident laser beam, μm; T is temperature, K; ρ_{20} is the electric resistance ratio of material at 20 ℃.

Owing to higher electric resistance of SiC compared with substrate, it can be known from the equation above that SiC ceramic phase preferentially absorbs heat first and is heated to a high temperature rapidly by laser beam when the Al alloy surface is molten. Then the heat is transmitted to the surrounding region through heat conduction. This heating mechanism makes the temperature of SiC particle and material adjacent to it higher than that of the fused bath, so that the interface reaction is induced easily.

In the course of formation of SiC reinforced aluminium matrix composite surface, there is a critical value about the density of the laser irradiation energy. When the density of the laser irradiation energy is higher than this value, SiC particle will be molten in aluminium solution and there will be Al-C, Al-Si-C compound cementing out, as shown in Fig. 3. Fig. 4 illustrates XRD pattern of modified layer of SiC/6061Al MMC treated by laser. Analyses prove that the dentritic structure of thin pin is composed of Al_4C_3 and Al_4SiC_4 which have been mentioned in the paper of Hu and Baker[10]. The chemical equation can be expressed as follows:

$$4Al + 4SiC \rightarrow Al_4SiC_4 + 3Si$$
$$4Al + 3SiC \rightarrow Al_4C_3 + 3Si$$

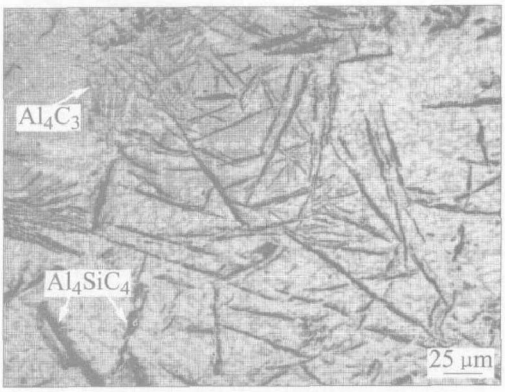

Fig. 3 Microstructure of Al_4C_3 and Al_4SiC_4 phase

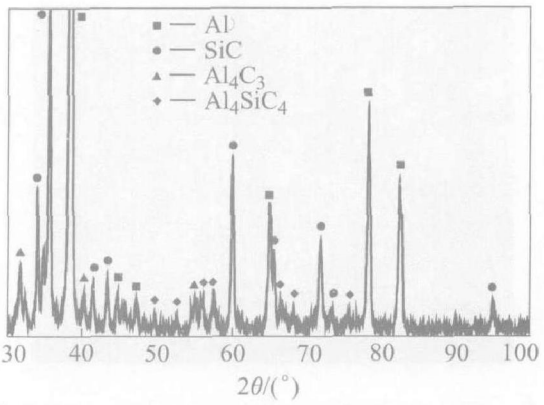

Fig. 4 XRD pattern of laser cladding surface

The product Si of the reaction mainly solidifies on the layer of aluminium alloy matrix.

3.2 Electrochemistry-corrosion performance of MMC modified layer

Fig. 5 shows the potentiodynamic polarization curves of as-received specimen and laser-cladded specimen in deaerated NaCl solution at 23 ℃. It can be concluded that, due to high volume fraction of the reinforced phase on laser processing surface, the corrosion-potential is increased by the use of laser-cladding technology to produce SiC particle reinforced MMC material layer (AA6061 Al E_{corr} = −1 293 mV, SiC_p/6061Al E_{corr} = −764 mV). Compared with AA6061 Al alloy, the passivity of the laser-cladded specimen decreases obviously. Fig. 6 shows the surface topography of pitting corrosion of electrochemical corrosion on laser cladding sample. The result shows that the interfaces

of Al/SiC, Al/Al_4C_3, Al/Al_4SiC_4 are the original sites of the pitting corrosion which provide more active sites for dull film. The inherent defect in dull film weakens the pitting corrosion resistance and the passivity of the MMC modified layer.

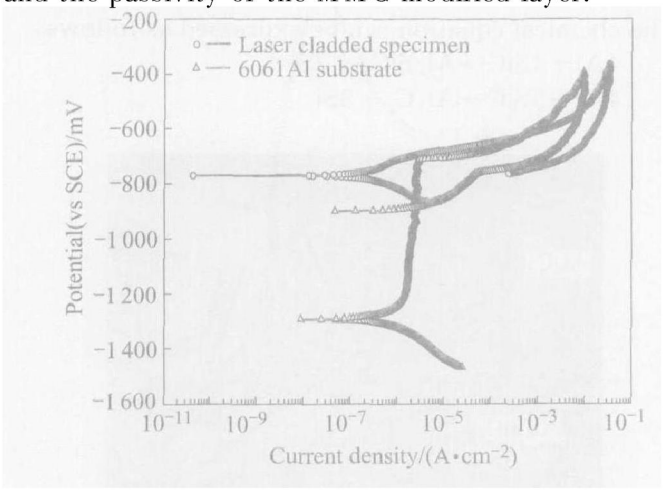

Fig. 5 Potentiodynamic polarization curves of substrate and laser-cladded specimens in deaerated NaCl solution at 23 ℃

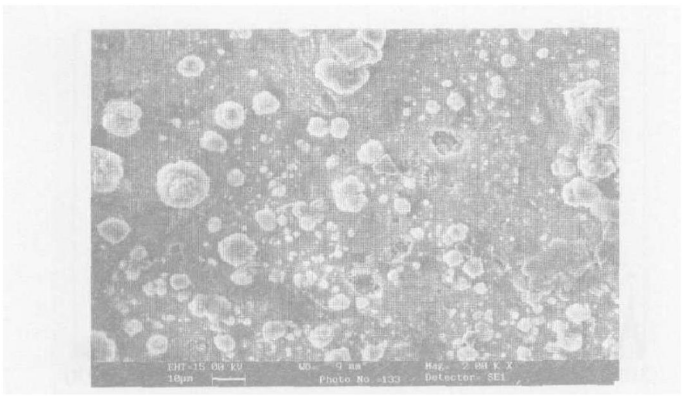

Fig. 6 Surface topography of pitting corrosion of electrochemical corrosion sample on laser cladding layer

3.3 Cavitation-erosion of MMC modified layer

3.3.1 Performance of cavitation-erosion resistance

Table 2 lists the cavitation-erosion rate and hardness of AA6061 Al alloy and laser cladded layer sample in 3.5% NaCl solution at 23 ℃. Compared with AA6061 Al alloy matrix, the specimen treated by laser losses fewer mass which can be explained by the fact that the modified layer of surface MMC material improves cavitation-erosion resistance of AA6061 Al alloy. According to Ref.[11], a given phase has a specific cavitation erosion mechanism and the erosion rate is controlled by its individual properties. For a multiphase material, the overall behaviour is a function of the respective contribution of each phase. The erosion rate can be described by the rule of mixtures, i.e. as a linear function of the volume fractions of the phases, i.e.

$$r = \sum \varphi_i r_i \quad (3)$$

where r is cavitation-erosion rate of the whole material; φ_i is the volume fraction of phase i; r_i is the cavitation-erosion rate of phase i.

Table 2 Cavitation-erosion rate and hardness of AA6061 Al alloy and laser cladded layer

Material	Erosion rate/(10^{-3} g·cm^{-2}·h^{-1})	$HV_{0.2}$
AA6061 Al substrate	7.49	56
Laser cladded layer	5.25	400－425

The whole volume fraction of SiC ceramic phase is a constant which benefits for cavitation-erosion resistance performance of AA6061 Al alloy because of high fracture toughness.

3.3.2 Cavitation-erosion damage mechanism

Fig. 7 shows SEM surface morphology of aluminium alloy matrix and laser-cladded specimens in 3.5% NaCl erosion media, respectively. The main cavitation-erosion inducing mechanism of the low hardness and mechanical strength of AA6061 Al alloy is surface-coarsening, mechanical hardening, necking and plastic fracture which lead material to move. Erosion-failure starts at interface of crystal grain. After being cavitation-eroded for 4 h, the grain of the aluminium appears as deep groove and necking fracture is the main mechanism in grain.

For the specimens cladded with SiC, their deformation mechanism is more complicated. In the

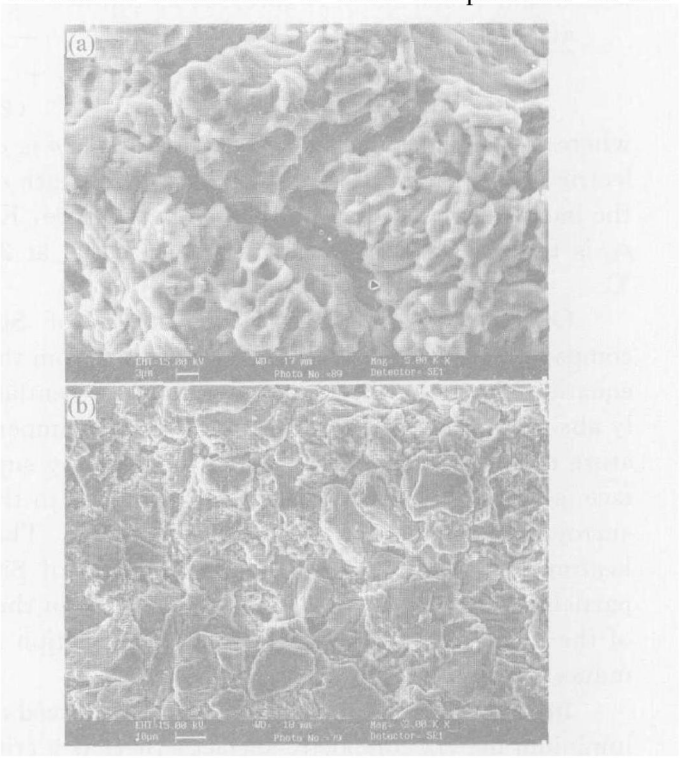

Fig. 7 Damage surface appearance after cavitation-erosive test for 4 h
(a) —AA6061 Al; (b) —Laser cladded sample

initial stage, the ceramics SiC in the matrix alloy are almost unaffected. The tiny pores and pits at the interface between the matrix and the ceramics provide sites of stress concentration, and erosion is initiated there. Since the aluminium matrix is much softer(Hv56) than the ceramics, work-hardening and fracture occur in the matrix preferentially. With the continuation of the damage, pits, work hardening and fracture as well as craters in the matrix increase. The adjacent craters merge into a large defect and the surface roughness increase. The craters do not occur in the hard ceramics phases because of their high fracture toughness and hardness. After the matrix around the ceramic phases is eroded, the ceramic phases such as SiC are removed away from the surface as individual debris.

4 CONCLUSIONS

1) By the method of laser-cladding, SiC particle reinforced MMC layer can be obtained. SiC particles have distributed uniformly in the cladded layer. A small amount of Al_4C_3 and Al_4SiC_4 intermetallic compounds appear on laser surface.

2) Because of the formation of pitting corrosion induced original sites at the interface of aluminium and ceramic (or intermetallics), pitting corrosion resistance and passivity of laser surface are decreased.

3) Because of SiC has higher fracture toughness compared with AA6061 Al alloy, the SiC particle reinforced MMC layer produced by laser-cladding improves the performance of cavitation-erosion resistance.

REFERENCES

[1] ZHANG Song, KANG Yu-ping, WU Wei-tao, et al. An in-situ formed TiC_p particle reinforcement composite coating induced by laser cladding on aluminium alloy [J]. Rare Metal Materials and Engineering, 2001, 30(6): 422-427. (in Chinese).

[2] ZHANG Chun-hua, ZHANG Song, MAN Hau-chung. Microstructure and cavitation erosion behaviour of laser surface cladding Ni-based alloy [J]. Journal of Iron & Steel Research, 2002(Special issue): 313-317.

[3] ZHANG Song, ZHANG Chun-hua, MAN Hau-chung, et al. Cavitation erosion performance of laser surface cladding MMC of Si_3Ni_4/AA6061 aluminium alloy [J]. Chinese Journal of Laser, 2003, 30(2): 185-188. (in Chinese).

[4] Kobayashi U K, Kojiro F. Laser cladding of intermetallic compound Al_3Ti on aluminum substrate [J]. Journal of Light Metal Welding and Construction, 1993, 31(4): 153-159.

[5] Chong P H, Man H C, Yue T M. Microstructure and wear properties of laser surface-cladded Mo-WC MMC on AA6061 aluminum alloy [J]. Surface and Coatings Technology, 2001, 145(1-3): 51-59.

[6] Richman R H, McNaughton W P. Correlation of cavitation erosion behavior with mechanical properties of metals [J]. Wear, 1990, 140(1): 63-82.

[7] ASTM. Standard Method for Conducting Cyclic Potentiodynamic Polarization Measurements for Localised Corrosion Susceptibility of Iron-, Nickel- or Cobalt-Based Alloys[S]. Annual Book of ASTM Standards Vol. 03. 02, Philadelphia, 1992.

[8] ASTM. Standard Method of Vibratory Cavitation Erosion Test[S]. Annual Book of ASTM Standards, Vol. 03. 02, Philadelphia, 1992.

[9] Duley W W. CO_2 Lasers: Effects and Applications [M]. New York: Academic Press, 1976. 136.

[10] Hu C, Baker T N. Laser processing to create in-situ Al-SiC_p surface metal-matrix composites [J]. Journal of Materials Science, 1995, 30(4): 891-897.

[11] Wei J, Wang F X, Cheng Y Q, et al. Cavitation erosion of cobalt alloy coatings containing tungsten carbide particles in hydrochloric and sulfuric corrosive media [J]. Journal of Tribology, 1993, 115(2): 285-288.

(Edited by YANG Bing)